

A Comprehensive Review of Weighted Change Vector Analysis Techniques for Forest Monitoring

Edgie Bajuyo

*Department of Computer Engineering
University of Science and Technology
of Southern Philippines
Cagayan de Oro City, Philippines
bajuyo.edgierose21@gmail.com*

Adriane Loquinte

*Department of Computer Engineering
University of Science and Technology
of Southern Philippines
Cagayan de Oro City, Philippines
adrianeloquinte@gmail.com*

Morrix Ohata

*Department of Computer Engineering
University of Science and Technology
of Southern Philippines
Cagayan de Oro City, Philippines
morrix.ken@gmail.com*

Abstract—In remote monitoring, real-time detection of forest disturbances is critical for effective environmental management and conservation. Weighted change vector analysis (WCVA) techniques have been considered promising methods to enhance detection accuracy by integrating the relative importance of different applicable spectral bands. While real-time vector change detection methods have been extensively studied, a comprehensive analysis and review is conducted on several correlating methods, particularly in regards to the imagery and vector analysis.

Five change detection methods and image analysis were particularly established for the review of vector analysis techniques. Then, these methods are subsequently analyzed, classified based on their underlying techniques, and evaluated for usability and performance in forest monitoring applications.

In this paper, we systematically review and compare existing methodologies in terms of accuracy and applicability across various remote sensing scenarios. The review not only systematically finds similar existing literature but also identifies research gaps and suggests for future improvement in weighted change vector analysis techniques. In general, our findings highlight that the integration of spectral weighting significantly enhances detection performance in forest monitoring, thereby providing a rigid framework for further methodological advancements and practical implementations in environmental monitoring.

Index Terms—forest monitoring, weighted change vector analysis, remote sensing, satellite imagery, near-infrared (NIR)

I. INTRODUCTION

Forest monitoring is critical for managing natural resources, and understanding ecosystem dynamics, as it helps in determining the general forest state and enables it to react to any changes to the forest at any given time [1]. In line with forest monitoring, the Traditional methods of vector analysis such as Change Vector Analysis (CVA) have been used for detecting changes over time from acquired multispectral satellite imagery. However, due to the Change Vector Analysis' reliance on normal spectral differences and fixed thresholds, it then often limits its sensitivity and accuracy in detecting changes over time especially in certain forest environments [2], [3].

Recent studies have introduced innovative approaches to overcome these limitations. The Direction-Dominated Change Vector Analysis (DCVA) [3] basically improves traditional or conventional CVA as it emphasizes their direction and incorporating the direction of change vectors

through clustering and adaptive thresholding which results in an improved detection of subtle forest disturbances within the specified area of detection [2], [3]. Similarly, [4] makes use of landslide mapping, a different area of expertise but regardless it correlates to forests' disturbances due to how landslides frequently occur as disasters. Through Object-Based Image Analysis (OBIA) and open-source tools, the study has demonstrated how segmenting high-resolution imagery into meaningful objects can enhance feature extraction and classification, even in complex terrain [4].

Recently, in operational monitoring, a near-real-time approach for forest disturbance detection using stochastic continuous change detection with Landsat time series has been developed. Development of a forest disturbance detection through the usage of continuous change detection algorithms [4], which dynamically adjust thresholds and capture rapid changes. Thus emphasizing the need for timely, responsive, less intensity monitoring systems. Some recent advances in deep learning, such as land-use/land-cover change detection have been quite the boon in terms of deep learning. The usage of weighted vectors enables the ability to produce highly accurate depictions of images as the thresholds becomes higher and more accurate [5], the proponents had leveraged high-resolution imagery and learning-based similarity measures to capture subtle changes that traditional methods such as the CVA might overlook.

Similarly, continuous change detection algorithms are used to adjust thresholds and capture rapid changes [3], [6]; however, this is applied to the Sentinel-2 time series to assess any damage to the forest when razed by a storm in areas around Italy. Thus highlighting the operational benefits of adaptive thresholding in event-specific monitoring scenarios similar to the proponent's study by detecting any forest disturbances [6].

Through these advances, this paper proposes a Simplified Weighted Change Vector Analysis (SW-CVA) approach that introduces a straightforward weighting mechanism to assign higher importance to the most informative spectral bands (e.g., the near-infrared band, critical for vegetation monitoring). Through the integration of these weighted spectral bands' differences, SW-CVA aims to enhance the detection accuracy of forest disturbances while maintaining computational efficiency—as stated in the studies to be a key consideration. This study not only positions SW-

CVA within the evolving remote sensing change detection methods but also correlates insights from diverse approaches to offer a robust and operationally viable solution for forest monitoring.

II. METHODOLOGY

In this study, we present a comprehensive framework for real-time forest disturbance monitoring through advanced remote sensing change detection techniques. Our methodology integrates and compares several vector change analysis approaches as well as several others that are in tandem with remote sensing. Additionally, each method offers unique advantages for detecting subtle spectral changes while addressing challenges such as threshold calibration, parameter tuning, and noise reduction.

By analyzing these methods in tandem, our approach not only benchmarks their similarities that are provided in Table 1, but is also designated with a detailed summary, their main focus, the mathematical tools employed, and key findings which is then presented on Table 2,

A. Change Vector Analysis

Change Vector Analysis (CVA) is a widely used technique for detecting and quantifying changes in multi-temporal data, particularly in remote sensing applications. The CVA technique is typically applied to pairs of images captured at different time intervals to identify regions where significant spectral changes have occurred [7]. By computing the difference vector between corresponding pixels across two images, CVA provides both the magnitude and direction of change, allowing for a more detailed understanding of how the forested areas have evolved over time. Other types of methods that make use of CVA that are present are Direction Change Vector Analysis (DCVA), Simplified Weighted Change Vector Analysis (SW-DCVA) and Weighted mean of Vectors.

Direction Change Vector Analysis (DCVA) focuses on the direction of change between multi-temporal feature vectors, often deemphasizing or simplifying the magnitude of change. By prioritizing directional shifts in spectral (or other feature) space, DCVA can more effectively capture subtle transformations in forested areas, such as changes in vegetation density or structure [3]. Consequently, DCVA has been successfully applied to forest change detection as shown in Fig. 1 by analyzing between pairs of images, thus reducing the confounding effect of large brightness or magnitude differences in the data.

Simplified Weighted Direction Change Vector Analysis (SW-DCVA) builds upon the concept of DCVA by incorporating a weighting scheme to emphasize certain features, bands, or indices [5], [7]. This approach is particularly useful when prior knowledge indicates which spectral regions or variables are most relevant to the phenomenon under study. Weighted mean of vectors algorithm [5] can optimize detection performance by selectively amplifying or reducing certain dimensions where certain spectral bands may be more indicative of vegetation health or stress.

Fig. 1 is an example of a dataset acquired from a specific area within a country. (a) is the location of the study, (b) are the Sentinel-2A images acquired in Chengde, (c) are the

Sentinel 2-A images acquired in Huangshan, and (d)-(f) are datasets 1-3, respectively.

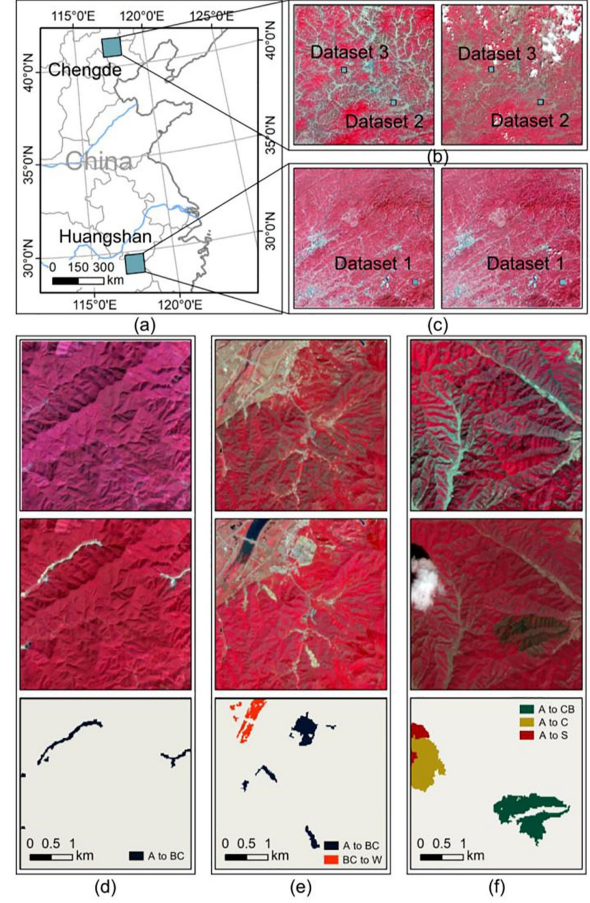


Fig. 1. Study Areas and datasets gathered from Sentinel-2A

Consider two multi-spectral images, X_1 and X_2 , each containing B spectral bands. For each pixel location (i, j) and band b , $X_{1,b}(i, j)$ and $X_{2,b}(i, j)$ denote the reflectance or intensity values. As shown in (1), the difference image X_D is then formed as:

$$X_{D,b}(i, j) = X_{2,b}(i, j) - X_{1,b}(i, j), \quad (1)$$

Here, $X_{1,b}$ and $X_{2,b}$ represent the values in bin b for two different data sets, while $X_{D,b} = X_{2,b} - X_{1,b}$ forms the difference vector CV . The integer B is the total number of bins (or dimensions). (2) defines ρ as the Euclidean norm of CV , indicating the overall magnitude of the difference between the two data sets. (3) defines θ as the direction (or angle) associated with that difference, reflecting how the net shift is oriented. Together, ρ and θ provide a compact representation of the change: ρ quantifies the extent of the discrepancy, while θ indicates its orientation. This polar-like decomposition is especially useful for comparing or visualizing differences, as it condenses potentially high-dimensional information into a distance measure and an angle.

$$\rho = \sqrt{\sum_{b=1}^B (X_{2,b} - X_{1,b})^2} \quad (2)$$

$$\theta = \cos^{-1} \left(\frac{1}{\sqrt{B}} \left(\frac{\sum_{b=1}^B X_{D,b}}{\sqrt{\sum_{b=1}^B (X_{D,b})^2}} \right) \right), \quad \theta \in [0, \pi] \quad (3)$$

In the context of change detection, the terms TP, FP, FN, and TN refer to counts of correctly or incorrectly classified pixels. Specifically, TP (True Positive) is the number of changed pixels correctly identified as changes, FP (False Positive) is the number of unchanged pixels mistakenly labeled as changes, FN (False Negative) is the number of true changes missed by the method, and TN (True Negative) is the number of correctly identified unchanged pixels. These four quantities form the confusion matrix in classification tasks and serve as the basis for computing the precision, recall, F1-score, and accuracy metrics shown in (4), (5), (6), and (7).

$$\text{Precision} = \frac{TP}{TP + FP} \quad (4)$$

Equation (4) defines precision, which measures the proportion of correctly identified changes (TP) among all detected changes (TP + FP). A high precision value indicates a low rate of false positives, ensuring that most detected changes are indeed actual changes.

$$\text{Recall} = \frac{TP}{TP + FN} \quad (5)$$

Equation (5) represents recall, which quantifies the method's ability to detect actual changes by computing the fraction of correctly identified changes (TP) over the total actual changes (TP + FN). A higher recall means fewer missed detections.

$$F1 - \text{score} = 2 \times \frac{\text{Precision} \times \text{Recall}}{\text{Precision} + \text{Recall}} \quad (6)$$

Equation (6) expresses the F1-score, which is the harmonic mean of precision and recall. It provides a balanced measure that accounts for both false positives and false negatives. A higher F1-score suggests a well-performing model that does not overly prioritize either precision or recall.

$$\text{Accuracy} = \frac{TP + TN}{TP + TN + FP + FN} \quad (7)$$

Equation (7) defines accuracy, representing the overall proportion of correctly classified pixels (both changed and unchanged) over the total number of pixels analyzed. While accuracy is useful, it can be misleading in cases where the dataset is imbalanced.

McNemar's test [3], [8] is used to determine whether two classifiers (or methods) differ significantly in their accuracy on the same dataset. In the context of forest change detection, f_{12} is the number of samples misclassified by the first method but correctly classified by the second, while f_{21} is the number of samples correctly classified by the first method but misclassified by the second. The test statistic Z in (8) measures the magnitude of the difference $|f_{12} - f_{21}|$

relative to $\sqrt{f_{12} + f_{21}}$. A large $|Z|$ indicates a statistically significant difference in classification performance between the two methods, highlighting whether observed improvements (or declines) in forest change detection are unlikely to be due to chance.

$$Z = \frac{|f_{12} - f_{21}|}{\sqrt{f_{12} + f_{21}}} \quad (8)$$

DVCA places greater emphasis on the direction of change, while VCA considers both magnitude and direction equally [3], [9].

B. Weighted Mean of Vectors

The concept of weighted mean vectors for parameter estimation [5], presents an algorithm that assigns varying importance to different components within a search space. This approach can better handle complex optimization tasks, reduce premature convergence, and adapt to scenarios where certain variables (or spectral bands) hold greater significance. In the following sections, we adapt and refine the weighted mean of vectors algorithm to improve change detection accuracy and computational efficiency in forest disturbance analysis. Alongside DCVA and SW-DCVA, a *Weighted Mean of Vectors* approach [5] can also enhance detection performance by assigning different importance to certain spectral bands or features. (9) provides the general form of the weighted mean vector WM:

$$WM = \frac{\sum_{i=1}^N \mathbf{x}_i w_i}{\sum_{i=1}^N w_i}, \quad (9)$$

where $\{\mathbf{x}_1, \mathbf{x}_2, \dots, \mathbf{x}_N\}$ are difference vectors (e.g., spectral differences) and $\{w_1, w_2, \dots, w_N\}$ are the corresponding weights. For an *optimal explanation* with only two vectors, the weighted mean reduces to (10):

$$WM = \frac{x_1 w_1 + x_2 w_2}{w_1 + w_2}, \quad (10)$$

where x_1 and x_2 represent the two vectors (or values), and w_1 and w_2 are their respective weights. By emphasizing spectral dimensions strongly correlated with vegetation health or stress, while reducing the influence of less informative features, this algorithm can yield a more targeted representation of the overall change. As a result, the weighted mean method complements DCVA and SW-DCVA by providing an additional mechanism to prioritize critical bands or indices, ultimately refining forest disturbance detection.

Specifically, each weight (w_1, w_2, \dots, w_N) is determined by a wavelet function (WF) [5], a powerful tool for modeling seismic signals through compounding translations and dilations of oscillatory functions (e.g., mother wavelets). This wavelet-based approach ensures efficient fluctuations throughout the optimization process. The mother wavelet used here is shown in Fig. 2 and is defined by (11):

$$w = \cos(x) \times \exp\left(\frac{x^2}{\omega}\right), \quad (11)$$

where ω is the *dilation parameter*. By substituting this wavelet expression into the general weighted mean formulas

(9), (10) one can flexibly adjust each vector's influence according to its relevance for detecting forest disturbances.

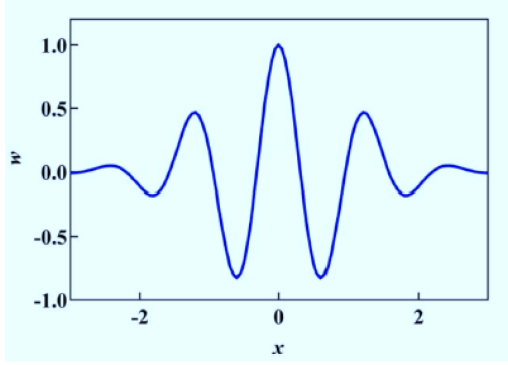


Fig. 2. Mother wavelet

In scenarios involving three vectors, (12), (13), (14), and (15) detail how to compute the weighted mean of those vectors. (12) derives WM by combining the pairwise differences $(\mathbf{x}_1 - \mathbf{x}_2)$, $(\mathbf{x}_2 - \mathbf{x}_3)$, and $(\mathbf{x}_1 - \mathbf{x}_3)$ with their respective wavelet-based weights w_1 , w_2 , and w_3 :

$$WM = \frac{w_1(\mathbf{x}_1 - \mathbf{x}_2) + w_2(\mathbf{x}_2 - \mathbf{x}_3) + w_3(\mathbf{x}_1 - \mathbf{x}_3)}{w_1 + w_2 + w_3}, \quad (12)$$

while (13), (14), and (15) define the weights themselves:

$$w_1 = \cos\left(f(\mathbf{x}_1) - f(\mathbf{x}_2)\right) \times \exp\left(\frac{(f(\mathbf{x}_1) - f(\mathbf{x}_2))^2}{\omega}\right), \quad (13)$$

$$w_2 = \cos\left(f(\mathbf{x}_2) - f(\mathbf{x}_3)\right) \times \exp\left(\frac{(f(\mathbf{x}_2) - f(\mathbf{x}_3))^2}{\omega}\right), \quad (14)$$

$$w_3 = \cos\left(f(\mathbf{x}_1) - f(\mathbf{x}_3)\right) \times \exp\left(\frac{(f(\mathbf{x}_1) - f(\mathbf{x}_3))^2}{\omega}\right), \quad (15)$$

where $f(\mathbf{x})$ represents the fitness function of vector \mathbf{x} , and ω is the dilation parameter used in the wavelet-based weighting. By leveraging wavelet-derived weights, this approach adapts to the significance of each vector in the overall optimization, offering a more flexible and targeted method for detecting changes or disturbances in the data.

C. Object-based image analysis

Object-Based Image Analysis (OBIA) segments imagery into meaningful objects based on spectral, spatial, and contextual properties, rather than analyzing individual pixels. This method helps to overcome the limitations of pixel-based approaches, particularly the "salt-and-pepper" effect, by leveraging groupings of pixels that represent real-world objects. OBIA has been successfully applied in various geospatial applications; The open source Semi-Automatic Landslide Detection system [4] demonstrated its effectiveness in landslide mapping using open source tools. Inspired by these findings, we correlate the usage of OBIA in the proponent's study to improve the classification accuracy and change detection in forested areas. Spectral, Topographical,

and Morphological features, refer to Fig. 3 for more details in regards to how these features are used.

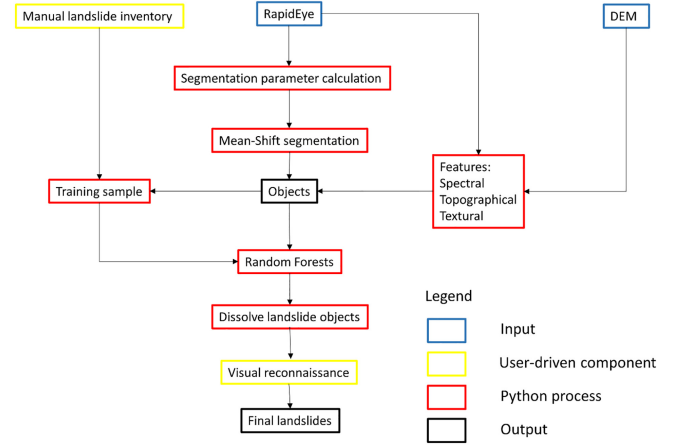


Fig. 3. SALaD system Flowchart

The SALaD system flowchart provides a comprehensive overview of the landslide detection process by integrating diverse data sources, user-defined parameters, and automated processing. Initially, input data—such as a manual landslide inventory [10], high-resolution RapidEye imagery [11], and a Digital Elevation Model (DEM) [12]—are gathered to supply both spectral and topographic information. The system then relies on user-driven segmentation parameter calculation to fine-tune the mean-shift segmentation algorithm, which clusters pixels into meaningful objects representing potential landslide and non-landslide areas. Each object is analyzed based on extracted features, including spectral reflectance [4], [13], topographical attributes [13]–[15] (like slope, aspect, and elevation), and morphological properties [4], [16] (such as area, perimeter, and texture). These features are subsequently fed into a random forest classifier to differentiate landslide objects from stable terrain [4].

Segmentations were then carried out in h_s of 10, h_r varying from 2 to 30 with a step size of 2 and minimum object size of 10 as image segmentation is crucial for producing objects that are considered homogenous and heterogenous. The intraobject homogeneity is calculated using weighted variance in (16).

$$v = \frac{\sum_{i=1}^n a_i v_i}{\sum_{i=1}^n a_i} \quad (16)$$

where a_i and v_i are the area and intraobject variance of segment i , respectively. Moran's I index [11] [17] is expressed as

$$I = \frac{n}{S_0} \times \frac{\sum_{i=1}^n \sum_{j=1}^n w_{ij} z_i z_j}{\sum_{i=1}^n z_i^2} \quad (17)$$

where z_i is the deviation of the brightness value of object i from its mean $x_i - \bar{X}$. $w_{i,j}$ is the spatial weight

between objects i and j , which is 1 for adjacent regions or 0 otherwise, n is the total number of objects, and S_o is the aggregate of all spatial weights. (18) defines S_o as follows:

$$S_o = \sum_{i=1}^n \sum_{j=1}^n w_{i,j}, \quad (18)$$

The objective function is defined in (19):

$$F(v, I) = F(v) + F(I), \quad (19)$$

Functions $F(v)$ and $F(I)$ are normalization functions, as shown in (20):

$$F(x) = \frac{X_{max} - X}{X_{max} - X_{min}}, \quad (20)$$

The POF is created using (21):

$$F(plateau) = F(v, I)_{max} - \sigma, \quad (21)$$

where $F(v, I)_{max}$ is the maximum value and σ is the standard deviation of the objective functions calculated from varying h_r .

Conceptually comparing these systems reveals similarities in their detection methods, as one approach focuses on landslides in their entirety, while the other addresses minor to major disturbances within forests. In simpler terms, the OBIA approach leverages object properties and boundaries, whereas SW-VCA provides a more streamlined method for detecting disturbances.

D. Continuous Change Detection Systems

Continuous change detection systems enable near real-time monitoring of environmental changes by continuously analyzing dense time series data, rather than relying on isolated snapshots. This approach captures both abrupt disturbances and gradual trends in land cover, offering a more comprehensive understanding of dynamic landscapes.

Continuous change detection algorithms (CCD) to Sentinel-2 imagery [6], demonstrating the method's capability to capture transient, rapid events. Similarly, a stochastic continuous change detection framework using Landsat time series effectively identifies subtle, early-stage disturbances in forested areas. By integrating these advanced techniques, continuous change detection systems not only enhance the timeliness of disturbance detection but also improve the overall accuracy of environmental monitoring, thereby supporting more proactive management strategies shown in Fig. 4

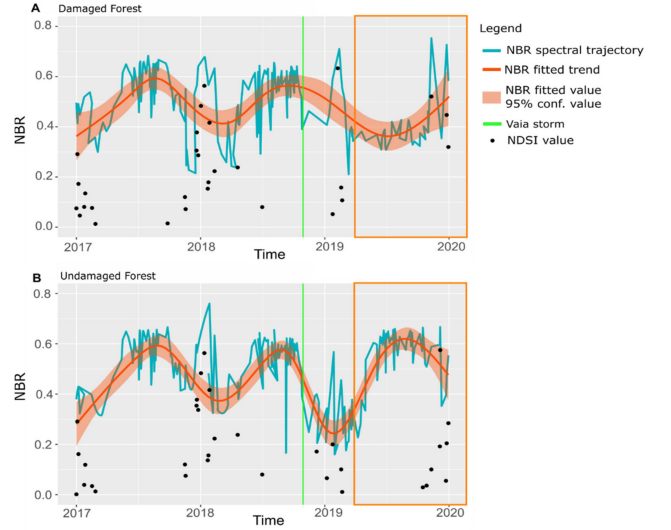


Fig. 4. Example of NBR spectral trajectories analysis of two different forest areas

Two forested areas—one affected by a storm (Panel A) and one undamaged (Panel B)—using the Normalized Burn Ratio (NBR) [6]. The damaged forest exhibits a pronounced drop in NBR following the storm, indicating stress or loss of canopy, whereas the undamaged area remains relatively stable over the same period. Cloud and shadow pixels were masked out using an appropriate algorithm (e.g., Fmask), ensuring that the analysis focuses on valid observations. To confine the study to forested regions, high-resolution masks were applied based on the FAO forest definition.

Additionally, the NDSI (Normalized Difference Snow Index), SWIR's 1 and 2 (Short-Wave Infrared), computed as

$$NDSI = \frac{Green(S2 - Band3) - SWIR(S2 - Band11)}{Green(S2 - Band3) + SWIR(S2 - Band11)} \quad (22)$$

can be employed to assess snow or certain reflectance changes, although the key takeaway in this figure is the temporal shift in NBR for the damaged area. Results demonstrate the utility of spectral indices for near-real-time disturbance monitoring and highlight the clear contrast between disturbed and undisturbed forest dynamics [6].

Stochastic Continuous Change Detection (S-CCD) is a time series analysis method designed to identify abrupt or gradual changes in remote sensing data [6], [18]. By incorporating probabilistic modeling, it can better distinguish real disturbances from noise or seasonal fluctuations. Typically, S-CCD monitors spectral indices (e.g., NBR, NDVI) over time, enabling near-real-time detection of forest disturbances or other land cover shifts. This approach is especially useful for large-scale monitoring, where rapid and accurate change detection is critical for timely decision-making. The S-CCD workflow comprises of three main stages: data preparation, model initialization, and continuous monitoring in Fig. 5.

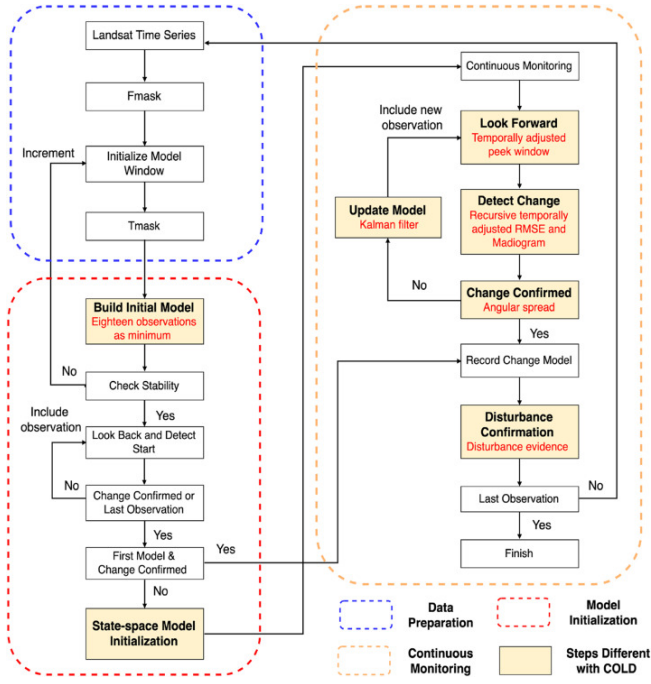


Fig. 5. Workflow of the Proposed Stochastic Continuous Change Detection (S-CCD) system

The method begins with Data Preparation, where a Landsat time series [6], [18] is preprocessed to remove invalid observations using Fmask [12], [18], and an initial model window is selected. Next, Model Initialization creates a baseline state-space model—often requiring a minimum number of cloud-free images to ensure stability—while also checking for any early changes that may have occurred. Once the baseline is established, the system transitions to Continuous Monitoring, where each new Landsat observation is incorporated via a Kalman Filter [19] to update the model. Potential disturbances are flagged if metrics such as RMSE (Root Mean Square Error) [20] or Madiogram exceed predefined thresholds, and confirmed changes are recorded through a “change model” step. If enough evidence supports a significant deviation, the algorithm labels it as a disturbance, prompting a re-initialization of the baseline if necessary. This iterative process enables near real-time tracking of forest or land-cover changes by continually comparing observed reflectance against expected values derived from the baseline model.

The despiked NBR time series was decomposed into three components—trend, seasonal, and remainder—using the BFAST iterative algorithm [5]. The decomposition model is defined as (23).

$$Y_t = T_t + S_t + e_t, \quad (t = 1, \dots, d) \quad (23)$$

where Y_t are the observed data at time t , and T_t , S_t , and e_t represent the trend, seasonal, and remaining components, respectively. The total number of observations is denoted by d .

The trend component T_t is modeled as a piecewise linear function with slopes α_i and intercepts β_i in (24).

$$T_t = \beta_i + \alpha_i t \quad (\tau_{i-1}^* < t \leq \tau_i^*) \quad (24)$$

where $i = 1, \dots, s$ represents the segment index, τ_i^* are the breakpoints, and s is the number of breakpoints in the trend component.

The seasonal component S_t is modeled using a piecewise harmonic function (25).

$$S_t = \sum_{k=1}^K \left(\gamma_{j,k} \sin \left(\frac{2\pi kt}{v} \right) + \theta_{j,k} \cos \left(\frac{2\pi kt}{v} \right) \right), \quad (\tau_{j-1} < t \leq \tau_j) \quad (25)$$

where $j = 1, \dots, p$ represents the seasonal segment index, $\tau_j^\#$ are the break points in the seasonal component, and p is the number of break points. The variable K is the order of the harmonic function, which was set to 3 to accurately detect rapid forest changes such as double or triple changes in a year.

Cohen’s Kappa (K) [21] is a statistical measure used to evaluate the agreement between two classification results. It accounts for the possibility of agreement occurring by chance. The K value is computed using (26):

$$K = \frac{P_o - P_e}{1 - P_e} \quad (26)$$

where P_o represents the proportion of observed agreement, given by (27):

$$P_o = \frac{TP + TN}{TP + TN + FP + FN} \quad (27)$$

and P_e is the expected agreement, defined by (28):

$$P_e = \frac{((TP + FN) \times (TP + FP) + (TP + TN) \times (FN + TN))}{(TP + TN + FP + FN)^2} \quad (28)$$

The K value ranges between -1 and $+1$, where a higher value indicates stronger agreement beyond random chance, while lower values suggest weaker agreement.

TABLE I
COMPARATIVE ANALYSIS OF METHODOLOGICAL APPROACHES:
SIMILARITIES

Ref.	Approach	Similarities
[3]	Direction-dominated Change Vector Analysis [3]	The analysis of direction change vectors plays a crucial role in this study as it requires threshold calibration to distinguish genuine change from noise in which is necessary for the remaining studies.
[4]	Object-based Image Analysis [4]	Object-based Image analysis heavily relies on segmentation and object-delineation which emphasizes parameter tuning for optimal detection, similar to that of the calibration needs in other methods.
[18]	Landsat Time Series: Stochastic Continuous Change Detection [18]	Some studies implements a time-series approach for real-time monitoring due to the need for threshold setting and sensitivity adjustment to manage natural variability.
[5]	Weighted Mean of Vectors Algorithm [5]	Makes use of an algorithm as a weighting mechanism to enhance signal importance which adds a layer of threshold and sensitivity similarly to the other studies.
[6]	Time series Sentinel-2 imagery and Continuous Change Detection Algorithms [6]	Time series usually focuses on continuous monitoring using certain data in which this similarly demands calibration to handle subtle spectral variations and ensure reliable detection.

Table I mentioned the similarities among various methodological approaches used in recent remote sensing studies. The specific approaches may vary, however they all collectively signify the importance of change vector analysis in terms of remote sensing through highlighting their shared reliance on threshold calibration, segmentation/parameter tuning, and sensitivity adjustments. Despite differing in implementation and application focus, these approaches all emphasize the need to fine-tune detection parameters to reliably distinguish genuine changes from noise, thereby ensuring accurate and robust monitoring of forest disturbances.

TABLE II
SUMMARY OF 5 JOURNAL PAPERS

Paper Title	Focus	Mathematical Tools Used	Key Findings
Landslide Mapping Using Object-Based Image Analysis and Open Source Tools [4]	Selecting and tuning segmentation parameters in OBIA. Landslides vary in size, shape, and spectral characteristics; coarse settings merge features with the background, while fine settings lead to over-segmentation.	Plateau Objective Function (POF), topographic indices with multi-temporal data.	Improved delineation accuracy and reduced misclassification between landslides and stable terrain.
A Near-Real-Time Approach for Monitoring Forest Disturbance Using Landsat Time Series: Stochastic Continuous Change Detection [18]	Achieving the right balance between sensitivity and specificity. The algorithm must detect genuine disturbances early without triggering false alarms from noise, cloud cover, and seasonal variations.	Threshold selection via time-adaptive thresholding, structural time-series models with a Kalman filter.	Enhanced detection reliability that distinguishes genuine disturbances from transient spectral fluctuations.
Evaluation of Weighted Mean of Vectors Algorithm for Identification of Solar Cell Parameters [5]	Tuning parameter boundaries and designing an effective fitness function for a complex, high-dimensional, non-linear search space with multiple local optima and noisy measurement data.	Wavelet-based weighted mean.	Improved convergence accuracy and efficient parameter estimation in complex optimization tasks.
Direction-Dominated Change Vector Analysis for Forest Change Detection [3]	Determining an optimal global magnitude threshold to differentiate genuine forest changes from background variability, compounded by the challenge of selecting appropriate spectral bands from Sentinel-2A data.	Expectation-Maximization (EM) algorithm, spatial filtering, confidence-weighted reclassification, k-means clustering.	Enhanced change detection accuracy with reduced false positives and improved differentiation of forest disturbance types.
Estimating VAIADamaged Forest Area in Italy Using Time Series Sentinel-2 Imagery and Continuous Change Detection Algorithms [6]	Calibrating detection thresholds to identify subtle windstorm-induced damage while mitigating interference from natural variability, seasonal changes, and atmospheric effects.	Probability-based stratified estimators, multi-seasonal trend analysis, Cohen's Kappa assessment.	More reliable damage detection with increased confidence in damage area estimates and reduced impact of seasonal variability.

Table II presents a comparative summary of five journal papers, each addressing different challenges in remote sens-

ing, optimization, and change detection. While the specific focus of each study varies, they collectively emphasize advancements in algorithmic methodologies for analyzing geospatial and environmental data.

Despite employing distinct mathematical tools—ranging from probabilistic modeling and time-series analysis to adaptive thresholding and machine learning—the studies share a common objective: improving the accuracy and reliability of automated detection and classification systems. These shared methodologies highlight the broader significance of structured analytical approaches in remote sensing, optimization, and environmental monitoring.

III. CHALLENGES AND ISSUES

Challenges arise at multiple stages when using object-based image analysis (OBIA) and open-source tools for landslide detection. The primary challenge is the selection and tuning of segmentation parameters within the object-based image analysis (OBIA) framework [4]. Since landslides vary greatly in size, shape, and spectral characteristics, identifying the optimal range radius and minimum object size is critical. If the parameters are set too coarsely, distinct landslide features may be merged with the background; if set too finely, the resulting segmentation may become overly fragmented, complicating subsequent object merging and classification. This delicate balance in parameter calibration is essential to ensure that the OBIA approach can reliably delineate landslide boundaries using open-source tools.

A near-real-time monitoring system for forest disturbance detection using Landsat time series and a stochastic continuous change detection framework [18] has the main challenge that they are addressing is achieving the right balance between sensitivity and specificity: the algorithm must be sensitive enough to detect genuine disturbances early, yet robust enough to avoid excessive false alarms caused by inherent noise, cloud cover, seasonal variability, and other transient fluctuations in the data. This delicate trade-off requires careful calibration of detection thresholds and model parameters so that the stochastic framework can reliably distinguish significant changes from benign variations in the reflectance time series.

The implementation of the weighted mean from vectors algorithm (INFO) faces several issues. The definition of parameter boundaries and the design of the fitness function set the framework for the optimization process. Its main challenge [5] is optimally tuning the weighted mean of vectors algorithm to reliably estimate solar cell parameters. This involves selecting the appropriate parameter boundaries, scaling factors, and fitness function settings so that the algorithm can navigate a complex, high-dimensional search space with nonlinear behavior and multiple local optima, all while avoiding premature convergence and handling noisy measurement data.

A direction-dominated change vector analysis (DCVA) method presents challenges [3]. the main challenge lies in determining an optimal global magnitude threshold to distinguish genuine forest changes from background variability. If the threshold is set too low, the method tends to generate

false positives by misinterpreting minor spectral variations or noise as change. Conversely, setting it too high risks missing subtle but important disturbances in forest cover. The selection of appropriate spectral bands from Sentinel-2A data, which do not all contribute equally to change detection, further complicates implementation [3].

Applying continuous change detection algorithms (BFAST and CCDC) for mapping windstorm-damaged forest areas presents challenges [6]. Calibrating the continuous change detection algorithm to reliably identify windstorm-induced forest damage and this task is particularly difficult because the spectral signals of damage can be subtle and are often confounded by natural variability, seasonal changes, and atmospheric effects. Additionally, setting appropriate thresholds to differentiate between genuine damage and transient noise (e.g., due to clouds or illumination differences) is critical—too low a threshold may lead to false positives, while too high a threshold risks missing significant damage. Overcoming these challenges requires a careful balance of sensitivity and specificity, as well as robust preprocessing of the time series Sentinel-2 imagery to minimize interference from extraneous factors.

IV. SOLUTIONS

Optimizing object-based image analysis (OBIA) for landslide detection requires careful segmentation parameter tuning [4], which addresses the main challenge of selecting appropriate segmentation parameters. The Plateau Objective Function (POF) helps determine optimal thresholds, reducing over-segmentation and minimizing classification errors. Post-processing techniques, such as merging small objects and refining classification rules, further improve accuracy. Integrating topographic indices and multi-temporal data enhances feature selection, allowing better discrimination between landslides and stable terrain.

Enhancing stochastic continuous change detection for forest disturbances requires refining threshold selection and incorporating probabilistic modeling [18], which tackles the challenge of balancing sensitivity and specificity in disturbance detection. Time-adaptive thresholding dynamically adjusts detection limits based on seasonal variations and environmental noise. Additional filtering techniques, such as cloud masking and noise reduction models, minimize false positives. The inclusion of structural time-series models and the Kalman filter improves predictive performance, ensuring the algorithm distinguishes genuine disturbances from transient spectral fluctuations.

Improving the weighted mean from vectors algorithm (INFO) for solar cell parameter estimation focuses on refining the weighted mean computation process [5], which addresses the challenge of tuning parameter boundaries and avoiding premature convergence. Wavelet-based weighted mean adjustments enhance convergence accuracy while reducing sensitivity to noise. Adaptive parameter scaling ensures the algorithm effectively navigates complex, non-linear search spaces. Integrating statistical outlier detection methods reduces the impact of noisy measurement data on the final parameter estimates.

Refining the direction-dominated change vector analysis (DCVA) method for forest change detection requires improving threshold determination and classification accuracy [3], which directly tackles the issue of setting a global magnitude threshold. The expectation-maximization (EM) algorithm provides an adaptive approach for setting thresholds, reducing the likelihood of misclassification. Post-processing techniques, such as spatial filtering and confidence-weighted reclassification, further refine the detected changes. The k-means clustering method is used to classify change directions, improving the differentiation of forest disturbance types.

Enhancing continuous change detection algorithms (BFAST and CCDC) for mapping windstorm-damaged forest areas requires improved temporal modeling and validation techniques [6], which resolves the challenge of selecting the correct temporal window for accurate detection. Time-series analysis demonstrates that windstorm damage is best detected 7–12 months post-event when spectral differences stabilize. Probability-based stratified estimators refine damaged area calculations, increasing confidence in reported estimates. Incorporating multi-seasonal trend analysis reduces the influence of seasonal variability, while additional accuracy assessments, such as Cohen's Kappa agreement, ensure the robustness of classification results.

V. CONCLUSION

Advanced remote sensing applications can overcome domain-specific challenges through tailored, adaptive approaches. Optimizing OBIA for landslide detection is achieved by employing adaptive segmentation techniques that utilize the Plateau Objective Function to balance over-segmentation and fragmentation. Post-processing steps and the integration of topographic indices and multi-temporal data further enhance the discrimination of landslide features from stable terrain.

Stochastic continuous change detection for forest disturbances benefits from time-adaptive thresholding and probabilistic modeling, which help balance sensitivity and specificity by filtering out noise due to clouds, seasonal variability, and other transient fluctuations.

Similarly, the weighted mean from vectors algorithm for solar cell parameter estimation is improved through wavelet-based adjustments, adaptive scaling, and robust outlier detection, ensuring reliable navigation through complex, high-dimensional search spaces. In forest change detection, an adaptive thresholding approach based on the expectation-maximization algorithm—combined with k-means clustering and spatial filtering—refines change classification and minimizes false detections. For mapping windstorm-damaged forest areas, thorough time-series analysis and probability-based stratified estimators yield reliable estimates once spectral signals stabilize several months after the event.

Collectively, these solutions underscore the importance of adaptive parameter tuning, robust noise mitigation, and advanced modeling techniques. Future work should explore multi-sensor data integration and emerging machine learning methods to further enhance the accuracy and efficiency of these remote sensing approaches.

REFERENCES

- [1] A. Gessler, M. Schaub, A. Bose, V. Trotsiuk, R. Valbuena, G. Chirici, and N. Buchmann, "Finding the balance between open access to forest data while safeguarding the integrity of national forest inventory-derived information," *New Phytologist*, vol. 242, no. 2, pp. 344–346, 2024.
- [2] H. Fang, P. Du, X. Wang, C. Lin, and P. Tang, "Unsupervised change detection based on weighted change vector analysis and improved markov random field for high spatial resolution imagery," *IEEE Geoscience and Remote Sensing Letters*, vol. 19, pp. 1–5, 2021.
- [3] P. Xiao, G. Sheng, X. Zhang, H. Liu, and R. Guo, "Direction-dominated change vector analysis for forest change detection," *International Journal of Applied Earth Observation and Geoinformation*, vol. 103, p. 102492, 2021.
- [4] P. Amatya, D. Kirschbaum, T. Stanley, and H. Tanyas, "Landslide mapping using object-based image analysis and open source tools," *Engineering Geology*, vol. 282, p. 106000, 2021.
- [5] A. Y. Hassan, A. A. Ismaeel, M. Said, R. M. Ghoniem, S. Deb, and A. G. Elsayed, "Evaluation of weighted mean of vectors algorithm for identification of solar cell parameters," *Processes*, vol. 10, no. 6, p. 1072, 2022.
- [6] F. Giannetti, M. Pecchi, D. Travaglini, S. Francini, G. D'Amico, E. Vangi, C. Coccozza, and G. Chirici, "Estimating via windstorm damaged forest area in italy using time series sentinel-2 imagery and continuous change detection algorithms," *Forests*, vol. 12, no. 6, p. 680, 2021.
- [7] L. Brand, *Vector and Tensor Analysis*. Courier Dover Publications, 2020.
- [8] M. Q. P. Smith and G. D. Ruxton, "Effective use of the mcnemar test," *Behavioral Ecology and Sociobiology*, vol. 74, pp. 1–9, 2020.
- [9] Y. Chen, "Spatial autocorrelation equation based on moran's index," *Scientific Reports*, vol. 13, no. 1, p. 19296, 2023.
- [10] G. Luetzenburg, K. Svennevig, A. A. Bjørk, M. Keiding, and A. Kroon, "A national landslide inventory of denmark," *Earth Syst. Sci. Data Discuss.*, pp. 1–13, 2021.
- [11] X. Zhang, L. Du, S. Tan, F. Wu, L. Zhu, Y. Zeng, and B. Wu, "Land use and land cover mapping using rapideye imagery based on a novel band attention deep learning method in the three gorges reservoir area," *Remote Sensing*, vol. 13, no. 6, p. 1225, 2021.
- [12] P. L. Guth, A. V. Niekerk, C. H. Grohmann, J. P. Muller, L. Hawker, I. V. Florinsky, and P. Strobl, "Digital elevation models: Terminology and definitions," *Remote Sensing*, vol. 13, no. 18, p. 3581, 2021.
- [13] F. Qamar and G. Dobler, "Atmospheric correction of vegetation reflectance with simulation-trained deep learning for ground-based hyperspectral remote sensing," *Plant Methods*, vol. 19, no. 1, p. 74, 2023.
- [14] E. Kalinicheva, D. Ienco, J. Sublime, and M. Trocan, "Unsupervised change detection analysis in satellite image time series using deep learning combined with graph-based approaches," *IEEE Journal of Selected Topics in Applied Earth Observations and Remote Sensing*, vol. 13, pp. 1450–1466, 2020.
- [15] A. C. Rodrigues, P. M. Villa, W. G. Ferreira-Júnior, C. E. R. Schaefer, and A. V. Neri, "Effects of topographic variability and forest attributes on fine-scale soil fertility in late-secondary succession of atlantic forest," *Ecological Processes*, vol. 10, pp. 1–9, 2021.
- [16] A. Srivastava, P. M. Saco, J. F. Rodriguez, N. Kumari, K. P. Chun, and O. Yetemen, "The role of landscape morphology on soil moisture variability in semi-arid ecosystems," *Hydrological Processes*, vol. 35, no. 1, p. e13990, 2021.
- [17] A. Shafique, G. Cao, Z. Khan, M. Asad, and M. Aslam, "Deep learning-based change detection in remote sensing images: A review," *Remote Sensing*, vol. 14, no. 4, p. 871, 2022.
- [18] S. Ye, J. Rogan, Z. Zhu, and J. R. Eastman, "A near-real-time approach for monitoring forest disturbance using landsat time series: Stochastic continuous change detection," *Remote Sensing of Environment*, vol. 252, p. 112167, 2021.
- [19] C. Urrea and R. Agramonte, "Kalman filter: historical overview and review of its use in robotics 60 years after its creation," *Journal of Sensors*, vol. 2021, no. 1, p. 9674015, 2021.
- [20] T. O. Hodson, "Root mean square error (rmse) or mean absolute error (mae): When to use them or not," *Geosci. Model Dev. Discuss.*, pp. 1–10, 2022.
- [21] G. Rau and Y. S. Shih, "Evaluation of cohen's kappa and other measures of inter-rater agreement for genre analysis and other nominal data," *Journal of English for Academic Purposes*, vol. 53, p. 101026, 2021.